Journal of Engineering Physics and Thermophysics, Vol. 79, No. 5, 2006

CALCULATION OF COMPRESSIBLE FLOW IN A SHORT VORTEX CHAMBER

V. V. Sorokin

UDC 532.527

A method for calculating a compressible turbulent flow in a short vortex chamber that incorporates calculations of the boundary layer at the end walls by the integral method and of the discharge by the theory of an ideal atomizer has been proposed. The magnitudes of pressure and circulation on the radius of the outlet orifice of the chamber, obtained in determining the boundary layer, have been used as input parameters in calculating the discharge, and the gas process has been regarded as isothermal. Favorable agreement between the calculated results and the experimental data has been found.

Consideration is given to a short vortex chamber (Fig. 1) comprising a lateral cylindrical generatrix 1 bounded by flat end walls 2 and 3, with the generatrix radius being larger than the distance between the end walls. On the lateral generatrix, guiding apparatus 4 (blades, slots, orifices, etc.) is located for injecting a gas and imparting the circumferential component of motion to it. In the center of one or both end covers, orifices 5 are made for gas escape. A short vortex chamber is the basic element of vortex valves, atomizers and sprayers, vortex mills, and reactors.

The flow in vortex chambers used in engineering is generally turbulent. The range of characteristic Reynolds numbers, based on the velocity in the slots of the guiding apparatus and the half-height of the chamber, is 10^4–10^5.

Methods for calculating the flow of an incompressible liquid in a short vortex chamber have been proposed in [1–3]. There is a semi-empirical method for calculating the flow of a compressible liquid in a vortex chamber [3]. It is characterized by an accuracy of 20–30% and has been developed mostly for long chambers.

Since the experimental modeling of vortex chambers encounters certain difficulties of scaling, the development of a method for calculating the flow in chambers with account for compressibility seems useful for engineering applications.

Description of the Flow Model. According to data of the visualization in a short vortex chamber, the radial gas flow is confined to boundary layers along the end walls, and the chamber is mainly occupied by a vortex, in which the level of radial velocities is low [1, 2].

A gas in the form of a narrow annular jet issues from the chamber through an orifice. Let us divide the steady axisymmetric turbulent gas flow into three regions a, b, and c with respect to the chamber radius (Fig. 1). The region of the developing flow (a) extends from the guiding apparatus $r = r_1$ to a certain radius $r = r^*$, which needs to be calculated. As a result of flows in the axial direction, the radial flow is localized in the end boundary layers, such that starting with r^* the radial velocity outside the boundary layer is absent. The region of the developed flow (b) stretches from $r = r^*$ to the radius of the outlet orifice r_2. The boundary layer and the vortex interact without transferring mass. The developing and developed flows are assumed to be symmetric to the midsection of the chamber. The discharge region (c) occupies the space from $r = r_2$ to $r = r_v < r_2$, where r_v is determined by calculation. The radial velocity of gas is absent, and the axial and circumferential velocities are significant.

Let the axial coordinate on the end wall of the chamber be $y = 0$ (Fig. 1). The continuity equation

$$\frac{\partial (\rho r u)}{\partial y} + \frac{\partial (\rho r w)}{\partial r} = 0 \tag{1}$$

Joint Institute of Power and Nuclear Investigations "Sosny," National Academy of Sciences of Belarus, 99 Academician A. K. Krasin Str., Minsk, 220109, Belarus; email: vnvv@sorokin.belpak.minsk.by. Translated from Inzhenerno-Fizicheskii Zhurnal, Vol. 79, No. 5, pp. 152–158, September–October, 2006. Original article submitted November 1, 2005.

1062-0125/06/7905-0999

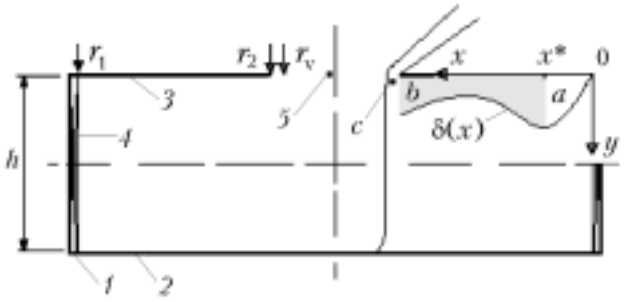

Fig. 1. Diagram of the vortex chamber and flow: 1) generatrix, 2 and 3) lower and upper end walls, 4) guiding apparatus, 5) orifices for gas escape; flow regions: a) developing flow; b) developed flow; c) discharge.

and the momentum equations for the boundary layer

$$\rho\left(u\frac{\partial u}{\partial r}-\frac{v^2}{r}+w\frac{\partial u}{\partial y}\right)=\frac{\partial \tau_r}{\partial y}-\frac{dp}{dr}, \tag{2}$$

$$\rho\left(u\frac{\partial v}{\partial r}+\frac{uv}{r}+w\frac{\partial v}{\partial y}\right)=\frac{\partial \tau_t}{\partial y} \tag{3}$$

with boundary conditions

$$y=0,\ \ u=0,\ \ v=0,\ \ w=0;\ \ y=h/2,\ \ w=0,\ \ \partial u/\partial y=0,\ \ \partial v/\partial y=0;$$

$$r=r_1,\ \ u=-u_0,\ \ v=v_0,\ \ w=0,\ \ p=p_0,\ \ \rho=\rho_0 \tag{4}$$

and with the equation of state of a gas

$$\frac{p+p_a}{\rho}=\frac{p_0+p_a}{\rho_0} \tag{5}$$

(p_a is the pressure at the chamber outlet) are sufficient for describing the gas motion at known τ in the regions of the developing and developed flows. Turbulence effects are allowed for by introducing shear stresses τ and characteristic velocity profiles. The transfer processes linked with density pulsations are not examined. The adopted assumption of isothermality of the gas process described by Eq. (5) can be qualitatively explained by the fact that the pressure drop mainly sustains the rotational motion in the chamber without leading to a noticeable flow acceleration and temperature decrease and the Mach number is smaller than unity.

We will solve problem (1)–(5) using the integral method of the boundary-layer theory. Let the boundary-layer thickness be $\delta = \delta(r)$. We specify the velocity profile [1]

$$0<y\le\delta\ \ u=-u_0\left(U(r)f(\eta)+U_s(r)\,g(\eta)\right),\ \ v=v_\delta(r)f(\eta);$$

$$\delta<y\le h/2\ \ u_\delta=-u_0U(r),\ \ v=v_\delta(r);\ \ \eta=y/\delta \tag{6}$$

and introduce the numbers

$$\alpha_1=\int_0^1 d\eta f^2,\ \ \alpha_2=\int_0^1 d\eta fg,\ \ \alpha_3=\int_0^1 d\eta g^2,\ \ \alpha_4=\int_0^1 d\eta g,\ \ \alpha_5=\int_0^1 d\eta f. \tag{7}$$

The functions f and g are assumed on the basis of experimental data, the quantities u_δ, u_s, and v_δ are determined from the solution of the system of equations; $u_s = u_0 U_s$ represents the secondary radial flow inside the boundary layer originating due to the pressure drop not compensated by the rotation.

Integrating Eq. (1) over the half-height of the chamber with allowance for expressions (4), (6), and (7), we obtain

$$\int_0^{h/2} dy \left\{\frac{\partial(\rho r u)}{\partial r}\right\} = \frac{d}{dr}\left(\int_0^{\delta} dy\{\rho r u\} + \int_{\delta}^{h/2} dy\{\rho r u\}\right) = -u_0 \frac{d\left(\rho r\left\{\delta(\alpha_5 U + \alpha_4 U_s) + (h/2 - \delta) U\right\}\right)}{dr} = 0$$

or, changing the differentiation variable $r \to x$ and introducing the designation $\underline{\delta} = 2\delta/h$, we get

$$\underline{\delta}'(\alpha_5 U + \alpha_4 U_s - U) + U'(1 - \underline{\delta} - \alpha_5\underline{\delta}) + U_s'(\alpha_4\underline{\delta}) = \left(\frac{1}{1-x} - \frac{\rho'}{\rho}\right)(\alpha_5 U\underline{\delta} + \alpha_4 U_s\underline{\delta} - U\underline{\delta} + U) \quad . \tag{8}$$

From expressions (1) and (4) we obtain the integral $w = -\frac{1}{\rho}\int_0^y dy\left(\frac{\partial(\rho r u)}{\partial r}\right)$. We next multiply Eq. (1) by u and add it to expression (2) multiplied by $r\rho$. Further on, we integrate the sum over the boundary-layer thickness with allowance for conditions (4), (6), and (7) and for the expression for w. Converting to dimensionless variables, we find

$$-\underline{\delta}'(\alpha_1 U^2 + 2\alpha_2 U U_s + \alpha_3 U_s^2 - \alpha_5 U^2 - \alpha_4 U U_s) - U'(2\alpha_1 U\underline{\delta} + 2\alpha_2 U_s\underline{\delta} - \alpha_5 U\underline{\delta}) -$$

$$- U_s'(2\alpha_2 U\underline{\delta} + 2\alpha_3 U_s\underline{\delta} - \alpha_4 U\underline{\delta}) = \frac{\alpha_1\underline{\delta}\lambda^2\underline{\Gamma}^2}{(1-x)^3} + \frac{1}{\rho}p'\underline{\delta} - \frac{2r_1\tau_r}{h\rho u_0^2} +$$

$$+\left(\frac{1}{1-x} - \frac{\rho'}{\rho}\right)\left(-\underline{\delta}(\alpha_1 U^2 + 2\alpha_2 U U_s + \alpha_3 U_s^2) + \underline{\delta}(\alpha_5 U^2 + \alpha_4 U U_s)\right), \tag{9}$$

where $\lambda = v_0/u_0$, $\underline{\Gamma} = v_\delta r/(v_0 r_1)$, $\underline{\rho} = \rho/\rho_0$, and $\underline{p} = p/(\rho_0 u_0^2)$.

Outside the boundary layer, Eq. (2) simplifies and in dimensionless variables gives

$$-UU' - \frac{\lambda^2\Gamma^2}{(1-x)^3} = \frac{1}{\rho}p'; \tag{10}$$

the same expression can be derived from Eq. (9), setting $\tau_r = U_s' = U_s = 0$ and $\alpha_1 = \alpha_5 = 1$.

After multiplying Eq. (1) by v and adding it to expression (3) multiplied by $r\rho$, we integrate the sum over the boundary-layer thickness with allowance for conditions (4), (6), and (7), and for the expression for w. Converting to dimensionless variables, we determine

$$\underline{\delta}'(\alpha_1 U + \alpha_2 U_s - \alpha_5 U - \alpha_4 U_s) + U'(\alpha_1\underline{\delta} - \alpha_5\underline{\delta}) +$$

$$+ U_s'(\alpha_2\underline{\delta} - \alpha_4\underline{\delta}) = -\frac{\delta(\alpha_1 U + \alpha_2 U_s)}{\underline{\Gamma}}\underline{\Gamma}' - \frac{2(1-x)\, r_1\tau_t}{\lambda h\rho u_0^2\underline{\Gamma}} +$$

$$+\left(\frac{1}{1-x} - \frac{\rho'}{\rho}\right)\underline{\delta}(\alpha_1 U + \alpha_2 U_s - \alpha_5 U - \alpha_4 U_s)\,. \tag{11}$$

Outside the boundary layer, Eq. (3) simplifies and in dimensionless variables gives

$$U\underline{\Gamma}' = 0 . \tag{12}$$

Equation (5) in dimensionless form becomes

$$\underline{\rho} = \frac{\underline{p} + \underline{p}_a}{\underline{p}_0 + \underline{p}_a} . \tag{13}$$

The boundary of the region of the developed flow $x^* = 1 - r^*/r_1$ is determined from the condition

$$U(x^*) = 0 . \tag{14}$$

After solving the system of equations (8)–(14) it is possible to calculate the Bernoulli constant H and the dimensional circulation Γ at $r = r_2$:

$$H = \left(\frac{p}{\rho} + \frac{\alpha_1 v_\delta^2}{2} \right)_{r=r_2} , \tag{15}$$

$$\Gamma = (\alpha_5 v_\delta r)_{r=r_2} . \tag{16}$$

In the discharge region there are no solid walls and wall friction. We assume that pressure drops are so insignificant that the gas compressibility can be disregarded. Then, in the discharge region the circulation and total pressure are retained, and the centrifugal force is offset by the pressure gradient

$$H = \frac{p}{\rho} + \frac{v^2 + w^2}{2} , \tag{17}$$

$$\Gamma = vr , \tag{18}$$

$$\frac{dp}{dr} = \frac{\rho v^2}{r} . \tag{19}$$

Expressions (17)–(19) imply that w = const, and the volumetric rate of flow of a liquid through the chamber is $Q = \pi \left(r_2^2 - r_v^2 \right) w$.

Let $r_v = \xi r_2$, $\xi < 1$. Using the condition of the maximum flow rate [2]

$$\frac{\partial H}{\partial \xi} = 0 , \tag{20}$$

we obtain a closed system of equations (15)–(20), which describes the flow in the discharge region. Transformed into dimensionless form, expressions (15)–(20) take the form

$$N = \frac{1}{\xi^2} + \frac{\Lambda^2}{(1 - \xi^2)^2} , \tag{21}$$

$$\Lambda^2 = \frac{(1 - \xi^2)^3}{2\xi^4} , \tag{22}$$

where $N = 2r_2^2 H/\Gamma^2$ and $\Lambda = Q/(\pi r_2 \Gamma)$ are dimensionless parameters. To describe the flow in the chamber, we choose, as in [1], the Blasius law of resistance, the velocity profile "1/7", and the initial values

$$C_f = 0.0225\,(2\nu/hu_0)^{1/4}, \quad \tau/\rho V^2 = 0.0225\,(\nu/\delta V)^{1/4}, \quad \tau_r = \tau\,(u/V), \quad \tau_t = \tau\,(v/V), \quad V^2 = v^2 + u^2;$$

$$f = (\eta)^{1/7}, \quad g = 1.69\,(1-\eta)^2\,(\eta)^{1/7};$$

$$\alpha_1 = 0.778, \quad \alpha_2 = 0.350, \quad \alpha_3 = 0.313, \quad \alpha_4 = 0.439, \quad \alpha_5 = 0.875;$$

$$\text{at} \quad x = 0.0005 \quad U_s = 0.686\lambda x^{1/2},$$

$$\underline{\delta} = \frac{36.2 C_f r_1 x^{1/2}}{h\lambda^{1/4}}, \quad U = \frac{1 + 0.439\underline{\delta} U_s}{1 - 0.115\underline{\delta}}.$$

The algorithm for calculating the rate of flow of a liquid through the chamber for a given pressure drop includes the specification of an approximate value of the flow rate Q_1, the calculation of the boundary layer in the chamber using Eqs. (8)–(14), the computation of the parameters N and Λ, and the finding of the flow rate Q_2 from relations (21) and (22). If Q_1 and Q_2 are dissimilar, the value of Q_1 is corrected and the calculation is repeated from the beginning. As soon as the coincidence of these values to an assigned accuracy is attained, the calculation is completed. Further on, it is possible to calculate the flow parameters of interest at any point of the chamber. If there are two outlets (in the upper and lower end covers), the calculation is carried out for the flow rate $Q/2$.

At fairly small radii of the orifices for gas escape from the chamber and high pressures at the inlet to the device, the values of the circumferential velocity inside the vortex chamber may reach a supersonic level. Generally, restricted supersonic flows change direction in a series of shock waves and rarefaction waves. However, the flow visualization in the chamber has not shown shock waves [4]. Since the flow is confined to the end boundary layer, in the current calculation it was assumed that a supersonic flow changes to subsonic in the isobaric hydraulic jump where the boundary layer thickness is increased by the jump and the velocity is decreased (Mach numbers are of the order of 0.99–1.01) such that the continuity equation is fulfilled. This does not contradict the visualization data and the laws of conservation, and it improves the calculation accuracy.

Comparison of Calculated Results and Experimental Data. We have obtained experimentally the flow rate characteristic of the vortex chamber with a single outlet and dimensions r_1 = 0.04 m, r_2 = 0.01 m, and h = 0.016 m, and a single tangential rectangular inlet with the cross section measuring 0.002 × 0.16 m. The chamber was blown through by compressed air, the air temperature in the receiver being 18°C. During the experiments, we measured the pressure on the radius r_1 at a corresponding rate of flow of air through the chamber. The pressure was determined by spring manometers of 0.6 accuracy rating with a measuring range of 0–0.25 MPa for low flow rates and 0–0.6 MPa for high flow rates. The chamber was placed in a high-capacity bunker connected to a damping section. As the latter, use was made of a straight channel with a diameter of 0.02 m for low flow rates and of 0.032 m for high flow rates, with a length of 46 and 32 calibers, respectively. At the inlet to the channels, flow-deswirling plates, each measuring three calibers, were installed. The flow rate was calculated from the maximum air velocity measured on the axis of the damping section by a Pitot–Prandtl tube. The pressure drop along the tube was measured with an accuracy of 0.001 m based on the difference in water levels in the arms of a U-shaped manometer. The air temperature was measured by a TK-5.03 thermometer (TEKHNOAS, Russia) with an attachment for determining the gas temperature with an accuracy of up to 1°C.

Figure 2 shows the rate of flow of air as a function of pressure at the inlet to the chamber. The results calculated with account for the hydraulic jump are in favorable agreement with the experimental data at excess pressures of at least up to 0.4–0.5 MPa, and with the hydraulic jump disregarded, at excess pressures of 0.3–0.4 MPa.

In [5], close consideration has been given to an air flow (20°C) in a chamber with a single outlet at r_1 = 0.142 m, r_2 = 0.0254 m, h = 0.032 m, v_0 = 26.4 m/sec, and u_0 = 2.64 m/sec; the guiding apparatus consisted of 48 blades located uniformly over the circumference. Blades were placed along the entire height of the chamber with the

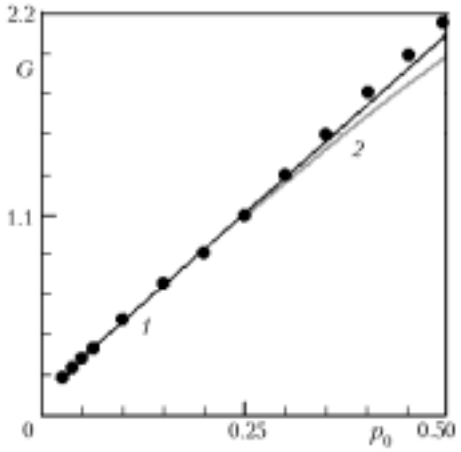

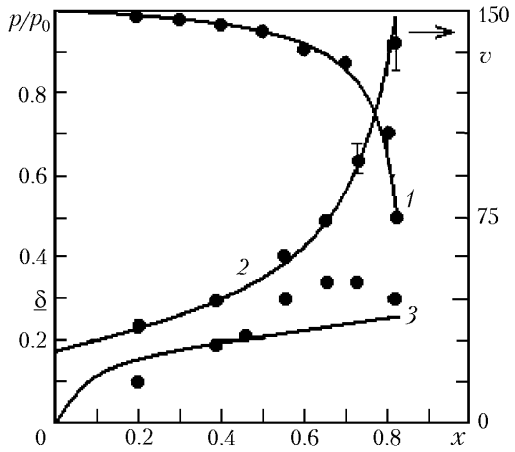

Fig. 2. Rate of flow of air as a function of the excess pressure at the chamber inlet: 1) theoretical dependence with account for the hydraulic jump; 2) same, with the jump disregarded; dots stand for experimental data. G, kg/min; p_0, MPa.

Fig. 3. Distributions of the static pressure p/p_0 (1), the circumferential velocity v (3), and the boundary-layer thickness $\underline{\delta}$ (2) along the chamber radius x: curves show calculated results and dots represent experimental data [5].

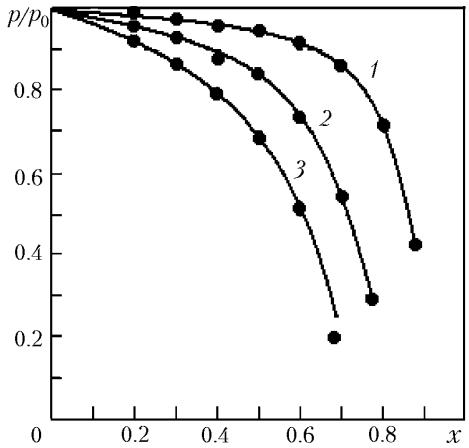

Fig. 4. Distributions of the static pressure p/p_0 along the chamber radius x: 1) r_2 = 0.0057 and $p(r_1)$ = 0.36, 2) 0.01 and 0.284, 3) 0.014 m and 0.22 MPa; curves represent results calculated at λ = 70, and dots show experimental data [6].

angle of inclination to the radius equal to 79° (practically tangentially). The velocity and pressure fields and the flow rates were measured at an inlet pressure of 0.142 MPa.

A comparison with the data of this study showed that the ratio of the calculated flow rate to the experimental one is 0.96. Figure 3 presents the distribution of static pressures, circumferential velocities, and boundary-layer thicknesses with respect to the chamber radius. The excess static pressure is based on the excess pressure on the radius r_1, and the boundary-layer thickness is referred to the half-height of the chamber. The pressure and velocity data are in favorable agreement. The measured velocity distribution near the outlet orifice turned out to be a function of the axial coordinate. The spread in the values of the function is bounded by vertical segments (curve 2). The agreement for the boundary-layer thickness is of a qualitative character, which may probably be in part attributed to the difficulties of the experimental determination of the boundary layer.

TABLE 1. Distribution of Dimensionless Pressure along the Chamber Radius

x	0	0.1	0.2	0.3	0.4	0.5	0.6	0.7	0.8	0.873
p_a	1	1	0.99	0.98	0.97	0.95	0.92	0.86	0.72	0.42
p_b	1	0.99	0.99	0.98	0.96	0.94	0.91	0.85	0.71	0.41
p_c	1	0.99	0.99	0.98	0.96	0.95	0.92	0.86	0.72	0.41

In [6], an air flow (20°C) has been investigated in a chamber with a single outlet at r_1 = 0.045 m, three values r_2 = 0.0057, 0.01, and 0.014 m, and h = 0.0125 m. The guiding apparatus consisted of four tubes with a diameter of 0.004 m, arranged uniformly over the circumference in the middle of the side wall. Tubes were positioned tangentially. The inlet pressures and the pressure distribution along the radius are known, and data as to the flow rate and the parameter λ are absent.

Selecting the value of λ by the criterion of closer agreement of the calculation with the experimental data on the pressure distribution along the radius for a chamber with r_2 = 0.0057 m, we obtain favorable agreement between experimental and calculated values for all r_2 (Fig. 4). In Fig. 4, the excess static pressure is based on the excess pressure on the radius r_1 (the absolute $p(r_1)$ is given in the figure captions).

The calculation shows that the dimensionless pressure distribution along the chamber radius is independent of the pressure at the inlet to the chamber. An example is presented in Table 1 (the chamber [6] has r_1 = 0.045 m, r_2 = 0.0057 m, and h = 0.025 m, and the subscripts refer to the absolute inlet pressures: a) 0.36 MPa, b) 0.26 MPa, and c) 0.16 MPa). This property is known from experiments [6, 7].

The proposed model satisfactorily describes the flow of a compressible liquid in a short vortex chamber and can be recommended for engineering applications.

NOTATION

f and g, functions specifying velocity profiles in the boundary layer; G, mass rate of flow of a liquid through the chamber, kg/sec; h, chamber height, m; p, static pressure at a current radius measured with respect to the pressure at the chamber outlet, Pa; Q, volumetric rate of flow of a liquid, m^3/sec; r, running radius, m; u, v, and w, radial, circumferential, and axial velocities of a liquid, m/sec; U, dimensionless radial velocity; $x = 1 - r/r_1$; y, axial coordinate, m; Γ, circulation, m^2/sec; δ, boundary-layer thickness, m; λ, parameter of the flow swirling; ν, kinematic viscosity of a liquid, m^2/sec; ξ, dimensionless radius of the vortex; ρ, density, kg/m^3; τ, shearing stress, Pa. Subscripts and superscripts: 0 and 1, on the chamber radius; 2, on the radius of the outlet orifice; δ, on the external boundary of the boundary layer; a, at the chamber outlet (the atmosphere); r, in the radial direction; t, in the circumferential direction; s, secondary radial flow; v, on the vortex radius; *, on the radius starting from which the entire radial flow passes through the end boundary layers; ′, derivative; underbar, dimensionless quantities.

REFERENCES

1. D. N. Wormly, An analytical model of an incompressible flow in short vortex chambers, *Trans. ASME*, *Ser. D*, *J. Basic Eng.*, No. 2, 145–159 (1969).
2. M. A. Gol'dshtik, *Vortex Flows* [in Russian], Nauka, Novosibirsk (1981).
3. I. I. Smul'skii, *Aerodynamics and Processes in a Vortex Chamber* [in Russian], Siberian Publishing House "Nauka," Novosibirsk (1992).
4. B. I. Zaslavskii and B. V. Yur'ev, Study of the flow structure in a flat vortex chamber, *Prikl. Mekh. Tekh. Fiz.*, **39**, No. 1, 84–89 (1998).
5. C. C. K. Kwok, Dihn Thinh Ngo, and Lin Sui, An investigation of confined vortex flow phenomena, *Trans. ASME*, *Ser. D*, *J. Basic Eng.*, No. 3, 181–188 (1972).
6. A. V. Antsupov and V. M. Mironov, Study of the aerodynamics of a vortex chamber, *Izv. SO Akad. Nauk SSSR*, *Ser. Tekh. Nauk*, No. 13, Issue 3, 26–32 (1981).
7. V. M. Glushchenko, Vortical liquid sprayer, in: *Vortex Phenomenon and Its Application in Technology* [in Russian], KuAI, Kuibyshev (1988), pp. 138–142.